

Classification of DCE-MRI Data for Breast Cancer Diagnosis Combining Contrast Agent Dynamics and Texture Features

Kai Nie¹, Sylvia Glaßer¹, Uli Niemann¹, Gabriel Mistelbauer¹, Bernhard Preim¹

¹Department of Simulation and Graphics, OvG-University Magdeburg
kai@isg.cs.uni-magdeburg.de

Abstract. Classification of breast tumors via dynamic contrast-enhanced magnetic resonance imaging is an important task for tumor diagnosis. In this paper, we present an approach for automatic tumor segmentation, feature generation and classification. We apply fuzzy *c*-means on co-occurrence texture features to generate discriminative features for classification. High-frequency information is removed via discrete wavelet transform and computation is simplified via principal component analysis before extraction. We evaluate our approach using different classification algorithms. Our experimental results show the performances of different classifiers with respect to sensitivity and specificity.

1 Introduction

In 2012, breast cancer was estimated in 1.7 million cases and 521,900 deaths world wide [1]. Dynamic contrast-enhanced magnetic resonance imaging (DCE-MRI) can characterize more details of breast tumors than standard MRI, through the contrast agents (CA) motion over time. In comparison with conventional X-ray mammography, DCE-MRI has higher sensitivity [2]. The average relative enhancement (RE) curve of a region of interest (ROI) reflects blood vessels and tissue permeability in this region. Based on the RE curve, Degani et al. presented the three-time-point (3TP) method [3], which allows for automatic classification of the RE curves. Glaßer et al. [4] clustered spatially connected tumor regions with similar 3TP classes to identify a "most suspect region" per lesion from which CA perfusion features were derived as input for the classification of malignant and benign breast tumors.

Data mining and machine learning have gained increasing popularity for benign and malignant tumors separation. Chang et al. [5] proposed to use co-occurrence texture features combined with kinetic curves to classify breast tumor types via fuzzy clustering. Zhang et al. [6] combined discrete wavelet transform (DWT) and principal component analysis (PCA) for feature extraction and classify brain images via a neural network (NN) classifier. Zheng et al. [7] used *k*-means to derive features from the membership probability of cluster that were learned on a set of malignant and a set of benign tumors, respectively. This reduced set of features was used for training the support vector machines (SVM) classifier.

We use fuzzy c-means (FCM) to generate new texture features based on the co-occurrence matrix, and combine with Gabor square energy and Gabor mean amplitude to improve the diagnosis in classifying breast tumors. The tumor region is segmented with the 3TP method. We employ three classifiers with the newly generated features and test their performance.

2 Material and Methods

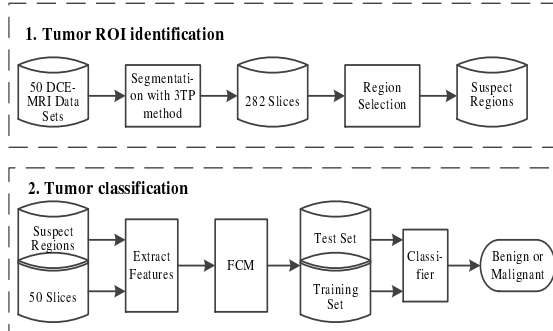
2.1 Image Data

In this study, we use a collection of 282 slices of tumor images from 50 patients, which include 141 slices of benign tumors and 141 slices of malignant tumors (see Preim et al. [8]). All data sets were acquired with a (rather old) 1T scanner (Philips Medical Systems) with the following parameters: matrix $\approx 500 \times 500$ pixels, slice thickness = 3 mm, slice gap = 1.5 mm, echo time = 6 ms, number of acquisitions = 5–6 s, total acquisition time = 300–400 s. We select 25 patients of benign tumors and 25 patients of malignant tumors from our data sets randomly. Each patient provides one slice breast tumor image, which can reflect typical traits of the tumor, and these 50 slices are used to establish the training sets after features extraction. All these images have already been segmented by an expert radiologist.

2.2 Methods

Fig. 1 shows the general steps of the presented approach, which is separated into two parts: tumor region of interest (ROI) identification and tumor classification.

Fig. 1. The workflow of the presented approach.



The temporal features of the DCE-MRI data can effectively distinguish lesions from normal tissue. Thus, we segment the data via the 3TP method. The 3TP method [3] provides an automatic classification of the tumor’s perfusion characteristics based on the RE curve. The RE is calculated with $RE = (SI_c - SI)/SI \times 100$, where SI is the pre-contrast and SI_c is the post-contrast

signal intensity [2]. We extract the three time points t'_1 , t'_2 , t'_3 , where t'_1 is the first time point before contrast agent injection, t'_2 is 2 min after t'_1 and t'_3 is 4 min after t'_2 . Fig. 2 shows the RE curves classification via the 3TP method. At t'_2 the RE curve is classified into three types: slow, normal and fast. If the result is normal or fast, the lesion areas will be identified as suspicious and be segmented. We use 3×3 median filter and bilateral filter to reduce noise. Meanwhile, the texture features have strong relationship with the size of image and the position of lesion, therefore we use rectangular ROIs to select the regions and remove the background.

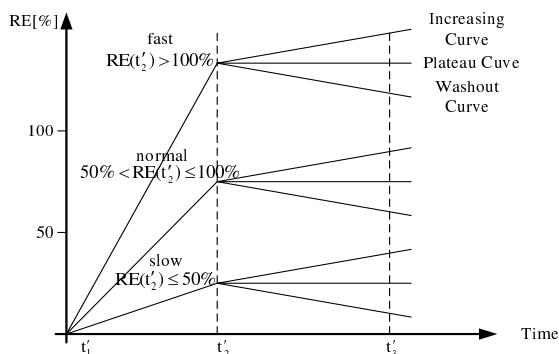


Fig. 2. The three-point method for evaluating DCE-MRI data (adapted from [3]).

We use two level discrete wavelet transform (DWT) to capture the frequency characteristics of the tumor ROIs and use principal component analysis (PCA) to reduce the number of dimensions. We remove high-frequency detail information and simplify computation via two level DWT and PCA. We extract 12 features, including contrast, correlation, energy, homogeneity, mean, standard deviation, entropy, root mean square, variance, smoothness, kurtosis, skewness, inverse difference moment, from the tumor image using the gray-level co-occurrence matrix (GLCM) method combined with Gabor square energy and Gabor mean amplitude.

In k-means clustering, each data point is assigned to exactly one cluster. We choose its extension, FCM, where the degree of cluster membership is given as probability. We employ FCM to extract malignant and benign tumor features separately, as described in [7]. We extract the features from training sets and recognize their patterns, which reflect the average distance of each feature to its cluster centroid. After this, we measure the similarity of each feature of the test sets and the detected patterns via FCM, which shows how well the features are fitted. For each feature, the clustering result reflects its effectiveness in classification. If the result is < 0.3 in both malignant and benign measurement, this feature is considered as irrelevant and is removed.

We assess the performance of the subsequent classifiers: decision tree C4.5, support vector machine with a linear kernel and radial basis function (RBF)

kernel, probabilistic neural network. We use the new features sets to learn these classifiers.

3 Results

In this section, we study the performance of the 3TP segmentation methods, the impact of the ROI selection and the performance of different classifiers. Our implementation is done in Matlab 2015a on a Windows 7 platform with an Intel Core i5 CPU at 3.3GHz and 8GB memory.

Fig. 3 shows two example tumors with different traits and shapes. Fig. 3(a) depicts a benign tumor with an irregular shape and Fig. 3(d) depicts a regular malignant sample. Blue lines highlight the tumor boundaries. Fig. 3(b) shows the segmented result of a benign tumor, Fig. 3(e) shows the segmented result of a malignant tumor. Fig. 3(c) and Fig. 3(f) show the ground truth segmented by an experienced radiologist. The average 3TP segmentation accuracy is 98.2% for benign data and 98.3% for malignant data.

The proportion of the foreground pixel is calculated with $R = N_t/N_i$, where N_t is the number of foreground pixels, N_i is the number of the whole image pixels. Table. 1 shows the effect of the rate R on classification accuracy using probabilistic neural network (PNN) classifier. Thus, we set the rate R to 55%–60% for regular tumors and 50%–55% for irregular tumors, and all the lesions are set in the center of the regions to keep the classification result more stable.

The sensitivity and specificity are as follows: the sensitivity of decision tree C4.5, SVM with linear kernel, SVM with RBF kernel and PNN classifiers are

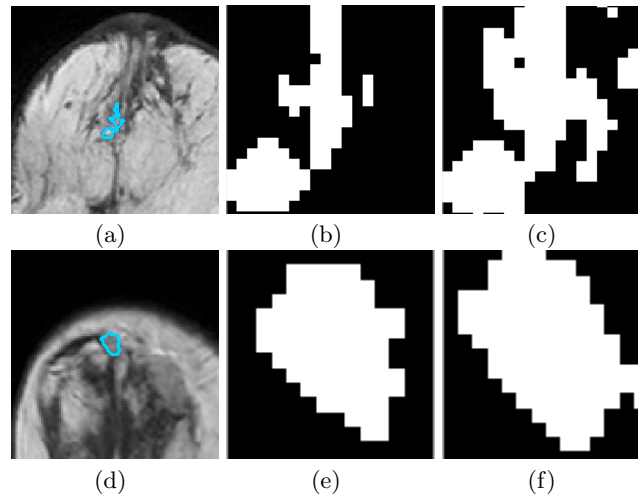


Fig. 3. Tumor segmentation result, (a) a benign tumor; (b) the segmented benign tumor; (c) the ground truth of the benign tumor; (d) a malignant tumor; (e) the segmented malignant tumor; (f) the ground truth of the malignant tumor.

Table 1. Classification accuracy of ROI selection using PNN Classifier.

Rate R		Classification accuracy (%)			
		< 50%	50%–55%	55%–60%	> 60%
Regular	Benign	87.6	90.5	93.3	94.3
tumors	Malignant	98.1	94.5	94.5	92.7
Irregular	Benign	86.1	91.7	94.4	94.4
tumors	Malignant	98.8	97.7	95.3	93.0

57.4%, 80.9%, 79.4% and 92.2%, the specificity are 63.1%, 97.2%, 98.6% and 95.8%, respectively.

Glaßer et al. [9,10] combined the 3TP method with J4.8 decision tree to classify the breast tumors, and the correctly classified instances are approximately 67% based on the same data set we use in this work.

4 Discussion

The 3TP method takes advantage of dynamic curves, which reflect the tissue’s pharmacokinetic characteristics or CA accumulation, to segment the suspected regions. Although the segmentation results can be easily obtained via the 3TP method, it is sensitive to artifacts, such as noise and tissue displacement, and time points selection.

Compared to the results of Glaßer et al. [9,10], we achieved a higher classification accuracy by integrating texture features. The combination of pharmacokinetic features and features representing the tumor’s texture enable a high accuracy even for this data with only moderate quality.

Despite the SVM having the highest accuracy in malignant tumor classification, the PNN classifier shows the best discriminative power among these three classifiers. Furthermore, the accuracy of classifying a tumor of benign is far below than the accuracy of malignant. The reason is that our data sets include numerous small tumors. These small tumors which can only be detected in DCE-MRI data, are very hard to distinguish and classify, even for a human expert, and these tumors have a substantial impact on the classification performance.

The ratio of foreground/background reflect the relationship between textural features and lesions. However, the ratio can not exceed a value cause the rectangular ROIs must include the whole lesion, and consider the diversity of data sets, the ratio should be set in a certain range. The influence of region selection on the classification result is shown in Table 1. Thus, we defined the size and position of ROIs before the classification, to reduced the impact of subjectiveness from manual region selection.

We presented a comprehensive workflow which includes feature extraction, feature selection and classification to separate between malignant and benign tumors in DCE-MRI data. 282 slices of tumor images, which had been confirmed as either malignant or benign, were considered in this study. We used the 3TP

method to segment the tumors, which provide a high accuracy. We could not eliminate all the errors in preprocessing and registering, which have influence on the segmentation. A total of 12 features are extracted and the invalid features are automatically removed by FCM. We compared different classifiers and concluded that the PNN classifier has a good performance in both benign and malignant tumors. Although the SVM shows the highest accuracy in malignant tumor classification, its poor stability for benign tumors does not make it suitable for small tumors with similar textures.

One limitation of our approach is the low classification accuracy for very small tumors. For future work, a hybrid classifier, improved segmentation methods, and the combination of temporal informations and textural informations will be taken into consideration. Then, the connectivity and correlation of tumors can be described, and the accuracy of tumor segmentation will be improved. Moreover, the combination of various features and classifiers ensemble can overcome the disadvantage of a single classifier.

References

1. Torre LA, Bray F, Siegel RL, Ferlay J, Lortet-Tieulent J, Jemal A. Global cancer statistics, 2012. *CA Cancer J Clin.* 2015;65(2):87–108.
2. Kuhl C. The Current Status of Breast MR Imaging Part I. Choice of Technique, Image Interpretation, Diagnostic Accuracy, and Transfer to Clinical Practice. *Radiology.* 2007;244(2):356–378.
3. Degani H, Gusic V, Weinstein D, Fields S, Strano S. Mapping pathophysiological features of breast tumors by MRI at high spatial resolution. *Nat Med.* 1997;3(7):780–782.
4. Glaßer S, Preim U, Tönnies K, Preim B. A visual analytics approach to diagnosis of breast DCE-MRI data. *Comput Graph.* 2010;34(5):602–611.
5. Chang RF, Chen HH, Chang YC, Huang CS, Chen JH, Lo CM. Quantification of breast tumor heterogeneity for ER status, HER2 status, and TN molecular subtype evaluation on DCE-MRI. *Magn Reson Imaging.* 2016;34(6):809–819.
6. Zhang Y, Dong Z, Wu L, Wang S. A hybrid method for MRI brain image classification. *Expert Syst Appl.* 2011;38(8):10049–10053.
7. Zheng B, Yoon SW, Lam SS. Breast cancer diagnosis based on feature extraction using a hybrid of K-means and support vector machine algorithms. *Expert Syst Appl.* 2014;41(4, Part 1):1476–1482.
8. Preim U, Glaßer S, Preim B, Fischbach F, Ricke J. Computer-aided diagnosis in breast DCE-MRI-Quantification of the heterogeneity of breast lesions. *Eur J Radiol.* 2012;81(7):1532–1538.
9. Glaßer S, Niemann U, Preim B, Spiliopoulou M. Can we distinguish between benign and malignant breast tumors in DCE-MRI by studying a tumor’s most suspect region only? *Proc of IEEE Computer-Based Medical Systems.* 2013; p. 77–82.
10. Glaßer S, Niemann U, Preim U, Preim B, Spiliopoulou M. Classification of Benign and Malignant DCE-MRI Breast Tumors by Analyzing the Most Suspect Region. *BVM.* 2013; p. 45–50.